On the Rational Design of Zeolite Clusters

Angela N. Migues,[†] Adina Muskat,[‡] Scott M. Auerbach,[†,‡] Woody Sherman,[§] and S. Vaitheeswaran*[,†,‡]

[†]Department of Chemistry, University of Massachusetts, Amherst, Massachusetts 01003, United States
[‡]Department of Chemical Engineering, University of Massachusetts, Amherst, Massachusetts 01003, United States
[§]Schrödinger Inc., 120 West 45th Street, New York, New York 10036, United States

S Supporting Information

ABSTRACT: We have applied density functional theory calculations to systematically investigate zeolite cluster-size convergence for two acid-zeolite-catalyzed processes related to the conversion of biomass: (1) the keto—enol tautomerization of acetone in HZSM-5 and HY and (2) the protonation and ring opening of furan in HZSM-5. We have used these reactions as platforms to study two different approaches for constructing successively larger cluster models of zeolites, with the aim of determining a protocol that converges the energy differences with minimal system size. One approach for cluster design involves counting framework bonds from the Brønsted acid-site aluminum atom. Another approach involves applying multicentered spherical cutoffs based on geometries of the zeolite active site, the adsorbed reactant, and the adsorbed product. We have investigated the convergence of reaction energies using single-point calculations on clusters containing as many as 166 tetrahedral (T) atoms and geometry optimizations on clusters with as many as 78 T atoms. For all reactions studied, convergence rates of single-point reaction energies agree well with those from geometry-optimized clusters. In addition, converged and optimized reaction energies agree well with previously published values for all reactions. Our central finding is that clusters generated with multicentered spherical cutoffs yield converged reaction energies with smaller system sizes than clusters generated by counting framework bonds. This method, employing a single length scale (5 Å), converges reaction energies with respect to system size to within chemical accuracy (±1 kcal/mol), and it includes between 15 and 34 T atoms in the cluster depending on the process and zeolite framework under investigation. We suggest a general protocol for generating such clusters for subsequent use in computational studies of zeolites and other heterogeneous catalysts.

KEYWORDS: zeolites, clusters, convergence, biomass, density functional theory, reaction energy
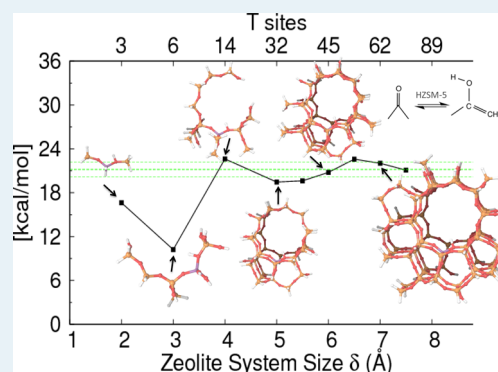
1. INTRODUCTION

Zeolites are crystalline microporous alumino-silicates that are widely used in industry as solid-acid catalysts due to their inherent shape-selectivity.[1,2] Zeolites are composed of tetrahedral subunits commonly denoted as TO_4 (where T = Al or Si).[3] The polar nature of the Si−O bond and the presence of charges in some zeolites can impose relatively strong electric fields on adsorbed guests, requiring care in computational treatments of long-range zeolite−guest interactions. Finite cluster models of zeolite crystals have nonetheless been extensively employed to understand reactive and adsorptive processes in zeolites of various framework types.[4] Convergence with respect to zeolite cluster size is possible despite the presence of long-range interactions, because the slowly varying, long-range contributions to reaction and activation energies—energy differences between nearby configurations—essentially cancel for large enough but finite cluster sizes.[5] It is not obvious, however, how large zeolite clusters need to be for such cancellation to occur. In the present article, we perform systematic computational tests on zeolite cluster models in search of simple rules that govern system-size convergence of zeolite−guest interactions.

Several alternative computational methods exist for treating long-range zeolite−guest interactions. Periodic density functional theory (DFT) codes such as VASP have proven useful for zeolites with small unit cells,[6−8] but calculations quickly become intractable for larger zeolites with, for example, FAU (e.g., zeolite HY) or MFI (HZSM-5) structure types.[2] The QM-Pot approach reported by Sauer and co-workers treats long-range interactions efficiently by mixing quantum and molecular mechanics (MM) calculations,[9,10] although this approach often relies on using DFT to parametrize the MM portion, which can be a cumbersome process. Other approaches for mixing quantum mechanics and force field calculations, generally denoted as QM/MM methods, have been applied to study reactions in zeolites.[11−15] However, QM/MM approaches may exhibit numerical instabilities when computing transition states,[15] potentially limiting their usefulness. In contrast, cluster calculations are relatively simple to apply to a wide range of zeolites.[16] Notably missing in the

literature is a systematic method for constructing optimal zeolite clusters. The challenge thus remains to determine optimal cluster sizes, and perhaps more importantly, to determine optimal methods for building optimal clusters.

In the present work, we address this issue by applying DFT to compute reaction energies for two processes relevant to the zeolite-catalyzed conversion of biomass: (1) the keto−enol tautomerization of acetone (Figure 1A), which is the rate-
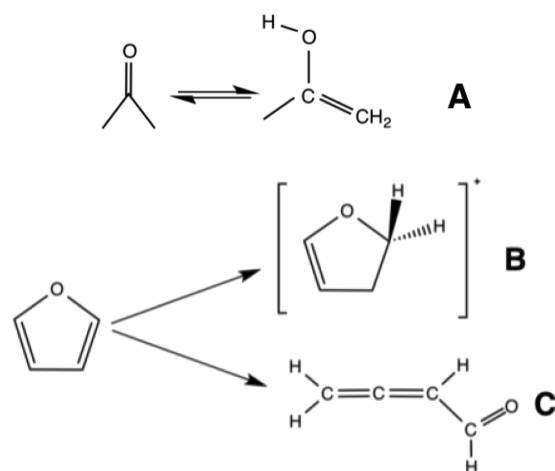
Figure 1. Reactions for (A) keto/enol tautomerization of acetone, (B) protonation of furan, and (C) ring opening of furan.

limiting step in aldol condensation,[4] and (2) the protonation and ring opening of furan (Figure 1B,C, respectively), which are initial steps in biofuel production via the catalytic fast pyrolysis of cellulose.[17,18] We focus herein on computing reaction energies instead of activation energies for the following two reasons: first, for computational ease as we consider below systems with as many as 166 T atoms; second, the insights from the present study extend to the convergence rates of activation energies as well. To see why, we note that when computing energy differences between nearby guest configurations, the convergence rate of the long-range component (arising from electrostatics) depends on how much the charge distributions differ—the greater the difference, the bigger the cluster required to converge the energy difference. Perhaps the most demanding case involves a neutral reactant that becomes a charged product (or vice versa). We have considered precisely this situation as shown in Figure 1B, and as such, our study elucidates the relevant aspects of zeolite cluster convergence for catalytic studies.

To investigate the issue of charge distributions, we consider a variety of reactions in Figure 1, including neutral → neutral and neutral → charged processes, to test whether the presence of charge influences convergence properties of zeolite clusters. We develop two distinct and simple approaches for rational construction of zeolite clusters. One approach pays homage to the anisotropic nature of zeolite structures, by counting framework bonds from a Brønsted acid-site aluminum atom. The other approach is based on including zeolite atoms that fall within multicentered spherical cutoffs and hence is more isotropic in nature. We demonstrate below that the approach using multicentered spherical cutoffs exhibits both smoother convergence and convergence at smaller system sizes. In addition, we find that a 5 Å cutoff is sufficient to converge a

variety of reaction energies as long as the cutoff is measured from all relevant reactant, product, and active-site atoms.

The remainder of this article is organized as follows: section 2 describes the systems under study and the methods for rationally building zeolite clusters; section 3 discusses the results and suggests a general approach for cluster construction; and section 4 offers concluding remarks.

2. METHODS

Reaction Processes. To elucidate the general principles that may guide cluster construction, we investigate four reactant−product pairs. The first two systems arise from the rate-determining step in the zeolite catalyzed aldol condensation between acetone and formaldehyde (Figure 1A).[4] These are the following:

1. Acetone (reactant) and enol (product) adsorbed in HZSM-5.
2. Acetone (reactant) and enol (product) adsorbed in HY.

In the final two systems, the reactant is furan adsorbed in HZSM-5. The products are the following:

3. Positively charged derivative of furan, protonated at the C2 position (shown in Figure 1B).
4. Neutral ring-opened species (shown in Figure 1C).

Both of these furan derivatives are key intermediates in the HZSM-5-catalyzed conversion of furan to benzofuran,[15] which leads to biofuel production via the catalytic fast pyrolysis of cellulose.

Zeolite Models. Guest molecule coordinates are taken from previously optimized clusters in our earlier studies.[4,15] Zeolite clusters are carved out from the periodic crystal, terminated at either Si or O, and capped with hydrogen atoms.[19,20] The Si−H bond lengths were set to 1.4 Å, while O−H bond lengths were set to 0.9 Å. As in our previous work,[4,14,15] the Brønsted acid site in HZSM-5 was chosen to be O(13), located at the intersection of the straight and zigzag channels. The HY cluster models were centered on O(1) in the 12-ring window with the Brønsted acid site pointed directly into the supercage. The applicability of the O(1) site as the Brønsted acid site was previously determined to be a catalytically relevant position.[5]

We have systematically expanded the zeolite clusters in the following two ways: (i) by counting framework bonds (so-called "n-bond" clusters) and (ii) by applying multicentered spherical cutoffs (so-called "delta" or "δ" clusters), as described below.

***N*-bond Clusters.** These clusters were constructed by including all framework atoms that are within n bonds from the Brønsted acid-site aluminum atom, where n ranges from 1 to 11 (illustrated in Figure 2 for $n = 3$ and 5). For relatively small clusters ($n \leq 3$), going from odd n to even n adds Si atoms, and from even n to odd n converts H-terminations to −OH terminations. This is seen in Figures 4C, 5A and 6A, in which increasing n from 2 to 3 for HZSM-5 keeps the number of T sites equal to 5. For larger clusters ($n \geq 4$), increasing n for HZSM-5 adds both Si and O atoms to complete rings to avoid overlaps of capping hydrogens. This method requires no *a priori* knowledge of guest molecule coordinates, and it guarantees the construction of well-connected zeolite clusters with no dangling atoms.

Delta (δ) Clusters. Alternatively, a zeolite cluster can be defined on the basis of proximity to the reacting atoms (e.g., relevant guest configurations and the Brønsted acid site). However, care must be taken to produce well-connected
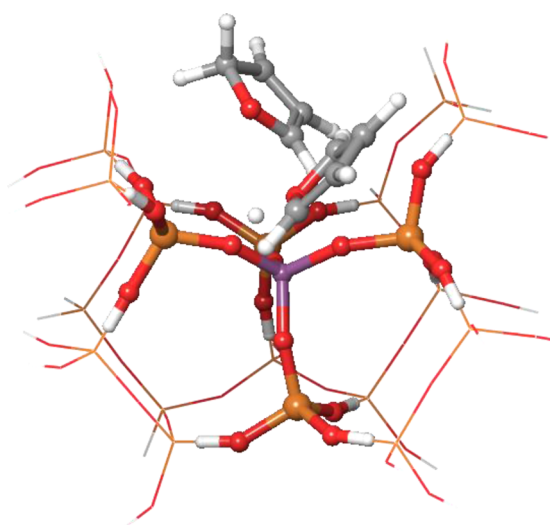
Figure 2. Illustration of an *n*-bond cluster of HZSM-5, where furan and protonated furan are shown as guest molecules. The *n* = 3 cluster is shown in ball-and-stick and the *n* = 5 cluster is shown as wire mesh (shown from the perspective looking down the intersection of the 10T straight and 10T zigzag channels).

clusters, as described below. In particular, the delta approach is based on the following two-step procedure: (i) include all zeolite atoms that fall within the union of several spheres—all with the same radius δ—but centered at the following various points: Brønsted acid site oxygen atoms, and each reactant and product guest atom (see Figure 3A). This approach requires initial guesses for adsorbed reactant and product geometries, which may be obtained relatively cheaply with low-level preoptimizations. (ii) If a framework atom A does not fall within the spherical cutoffs in step (i), but is bonded to two atoms that are included in step (i), atom A is included in the delta cluster. The delta method ensures that the cluster includes framework atoms that interact most strongly with the guest molecules. The final cluster used in computations is defined as the union set of all framework atoms selected in steps (i) and (ii) above (see Figure 3B). This procedure has been implemented systematically with an automated script using the Schrödinger Python API and is available from Schrödinger.

Computational Details. We seek to understand the convergence of long-range interactions in zeolitic host–guest systems with respect to zeolite cluster size. To this end, we calculate single-point energy differences between the product

and reactant states as a function of *n* and δ in *n*-bond and delta clusters, respectively. The single-point calculations ensure that atomic positions remain constant across clusters, hence providing rigorously comparable systems. Therefore, the cluster-size dependence of the energy differences can be solely attributed to the convergence of long-range interactions. This procedure has the added advantage of being fast enough that a large number of clusters can be evaluated to discern convergence trends. For example, a single-point calculation on the 78T HZSM-5 *n*-bond cluster required ~6 h, while an optimization on the same system required ~160 h. We also geometry-optimize selected clusters to confirm the relevance of the single-point energy differences, based on our previously published work on these reaction systems. In these optimizations, terminal −H and −OH groups were frozen in their crystallographic positions; all other atoms were free to move.

The B3LYP[21] hybrid density functional was used with the 6-311G(d,p)[22] basis set as implemented with the electronic structure program Jaguar.[23] This model chemistry has been previously shown by Fermann et al. to capture ~90% of activation energies for proton transfer processes in zeolites. Moreover, accurate barriers for the acid-catalyzed aldol chemistry were recently reported using this model chemistry.[4] We have determined the Gibbs energies of reaction in select delta clusters within the harmonic oscillator approximation, and have also implemented dispersion corrections using the Grimme[24] approach (reported in the Supporting Information); these were not found to influence the reported trends.

3. RESULTS AND DISCUSSION

Here we report the outcome of two different approaches for the rational construction of cluster models of zeolite crystals. First, we analyze and compare the differences between the two approaches for different reaction systems; (1) the keto/enol tautomerization of acetone in HZMS-5 and HY zeolites; (2) the protonation of furan; and (3) the ring opening of furan in HZSM-5. Then, we describe a general protocol for systematically constructing cluster models of zeolite crystals.

Acetone Tautomerization in Clusters of HZSM-5 and HY. The tautomerization of acetone in both HZSM-5 and HY follows a concerted mechanism and begins with the adsorption of acetone to the zeolite Brønsted acid site.[4] Once acetone is adsorbed, the zeolite acid site protonates the carbonyl oxygen while the adjoining methyl carbon is deprotonated, thereby regenerating the zeolite catalyst. Figure 4 shows single-point
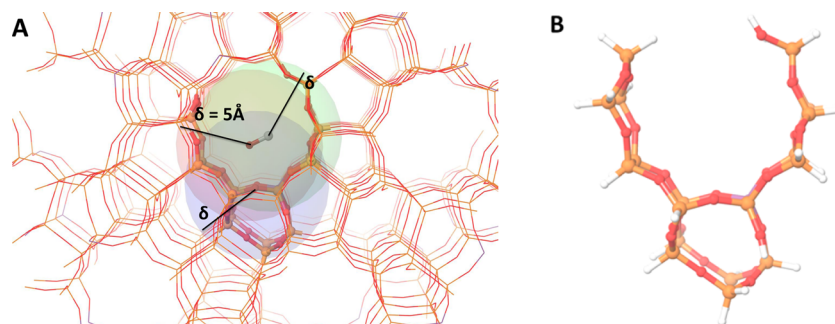
Figure 3. (A) Illustrated scheme for constructing delta cluster of HZSM-5 where carbon monoxide (CO) is used as an example guest molecule. The three spheres centered on guest C, guest O, and zeolite acid site O (all with the same radius, δ = 5 Å), are represented by different colors. The union set of the three spheres, plus four required connecting atoms (see text), yields the resultant delta cluster shown in (B), where CO has been removed for clarity, and dangling bonds have been capped with hydrogens.
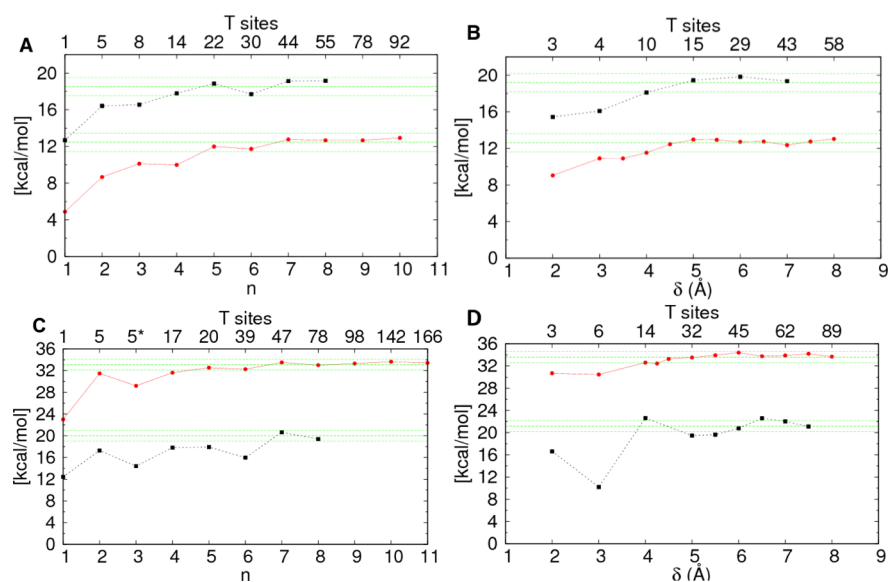
Figure 4. Dependence of reaction energies for the tautomerization of acetone in various size clusters of HY (A and B) and HZSM-5 (C and D); *n*-bond clusters (A and C) and delta clusters (B and D). All values shown in black correspond to optimized reaction energies and those in red to single point energy differences. In (C), the 5T cluster is −H terminated and the 5*T cluster is −OH terminated. The dashed green lines represent the zone of convergence to chemical accuracy (±1 kcal/mol).
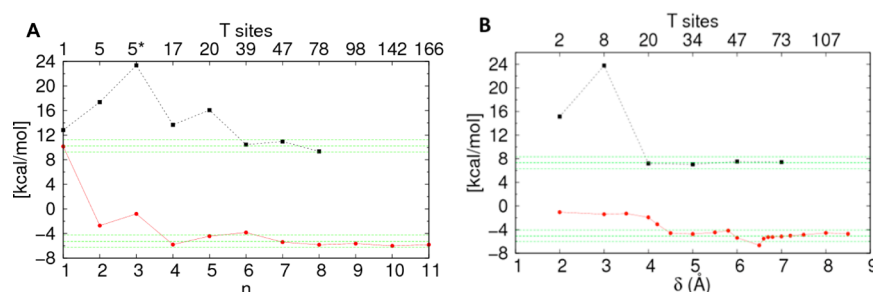
Figure 5. Dependence of reaction energies for the protonation of furan in various size clusters of HZSM-5; *n*-bond clusters (A) and delta clusters (B). In both (A) and (B), values shown in black correspond to optimized reaction energies and those in red to single-point energy differences. In (A), the 5T cluster is −H terminated and the 5*T cluster is −OH terminated. The dashed green lines represent the zone of convergence to chemical accuracy (±1 kcal/mol).

energy differences and optimized reaction energies for this reaction in both zeolites. Figure 4A,B demonstrate convergence for the HY *n*-bond and delta clusters, respectively. Figure 4C,D show the corresponding data for HZSM-5 *n*-bond and delta clusters, respectively.

In both zeolites, the converged single-point reaction energies using *n*-bond clusters agree well with the corresponding energies obtained using delta clusters. In Figure 4A, single point energies in *n*-bond clusters of HY converge to 12.0 kcal/mol when $n \geq 5$. The HY delta clusters mirror the same trend for the single-point energy differences (Figure 4B). When $\delta \geq 4$ Å, single-point energy differences converge to ∼12.2 kcal/mol (Figure 4B). In the case of HZSM-5, the single-point energies of the *n*-bond clusters converge to ∼33.0 kcal/mol for values of $n \geq 5$ (Figure 4C). This convergence trend is mirrored by the single-point energy differences in the delta clusters (Figure 4D). When $\delta \geq 4$ Å, energy differences converge to ∼33.5 kcal/mol in HZSM-5 (Figure 4D). Although the single-point energy differences converge to the same value with both approaches, it is important not to overinterpret the results of single-point energy calculations. Because single points do not provide optimized geometries, they are utilized only as a tool to gauge convergence of long-range interactions.

Optimized reaction energies of selected *n*-bond and delta clusters of HY and HZSM-5 reveal similar convergence trends with respect to system size (see Figure 4A,B and 4C,D). In *n*-bond clusters of HY and HZSM-5, reaction energies converge to 18.8 and 20.5 kcal/mol, respectively (Figure 4A,C). In delta-clusters of HY and HZSM-5, energies converge to ∼19.5 and 21.0 kcal/mol, respectively (Figure 4B,D, respectively). Both of our approaches to cluster construction yield optimized reaction energies in the two zeolites that agree well with the previously determined reaction energies at the same model chemistry.[4,25] Migues et al. reported 20.3 and 18.4 kcal/mol for a 30T cluster of HY and a 37T cluster of HZSM-5, respectively.[4] Boekfa et al. reported essentially identical results in a 34T cluster of HZSM-5.[25]

Although the two approaches converge to accurate reaction energies for both zeolites, they do not converge at the same system size. In fact, the optimizations reveal that the *n*-bond clusters of HZSM-5 do not converge until $n \geq 7$ (Figure 4C), which is a 47T cluster. In comparison, the delta clusters of HZSM-5 converge when $\delta \geq 4.0$ Å (Figure 4D); this system size corresponds to 14T. Similarly in HY, delta clusters converge at smaller system sizes compared to *n*-bond clusters. In Figure 4B, optimized reaction energies in HY converge when
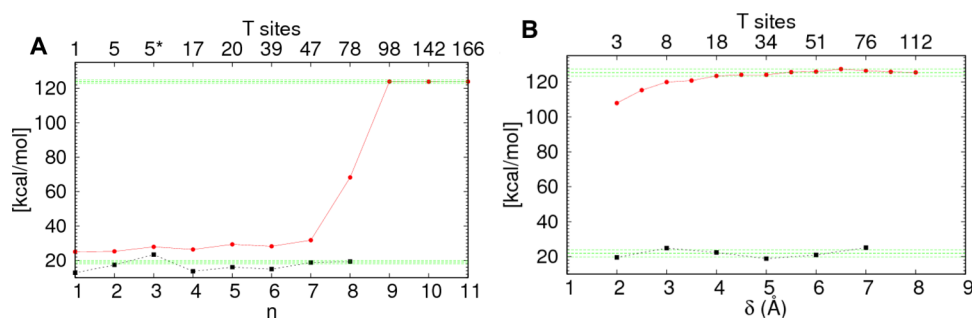
Figure 6. Dependence of reaction energies for the ring opening of furan in various size clusters of HZSM-5; n-bond clusters (A) and delta clusters (B). In both (A) and (B), values shown in black correspond to optimized reaction energies and those in red to single-point energy differences. In (A), the 5T cluster is −H terminated and the 5*T cluster is −OH terminated. The dashed green lines represent the zone of convergence to chemical accuracy (±1 kcal/mol).

$\delta \geq 4.0$ Å (10T) compared to n-bond clusters where convergence is not reached until $n \geq 4$ (14T). Our results demonstrate that clusters constructed using the multicentered spherical cutoffs converge reaction energies for the tautomerization of acetone in HZSM-5 and HY at smaller system sizes than the corresponding n-bond clusters.

Protonation of Furan in Cluster Models of HZSM-5. In this reaction, the Brønsted acid site in HZSM-5 donates a proton to an adsorbed furan at its C2 position, forming a positively charged intermediate.[15] Figure 5 shows single-point energy differences and optimized reaction energies for the protonation reaction of furan in n-bond (Figure 5A) and delta clusters (Figure 5B) of HZSM-5. Both methods of cluster construction agree reasonably well with each other.

In Figure 5A, single-point energies converge to ∼ −5.4 kcal/mol at values of $n \geq 7$ in HZSM-5. Optimizations reveal similar convergence trends at $n \geq 7$ with reaction energies of ∼10.0 kcal/mol (Figure 5A). Recall that $n = 7$ corresponds to a total system size of 47 tetrahedral units of HZSM-5. In Figure 5B, single point energies converge to ∼ −5.0 kcal/mol at $\delta \geq 4.5$ Å, and optimized energies converge to ∼7.2 kcal/mol at smaller values of δ ($\delta = 4.0$ Å). In this reaction system, a value of $\delta = 4$ Å corresponds to a system size of 20T.

Both of the approaches to cluster construction, n-bond and delta, yield reaction energies for the protonation reaction of furan that compare reasonably well to the previously reported value of 12.7 kcal/mol in HZSM-5.[15] In this previous study, an embedded (ONIOM) approach was followed using a 132T QM/MM cluster of HZSM-5, in which an 11T layer was treated quantum mechanically. Our results for the protonation of furan in HZSM-5 also demonstrate that delta clusters converge reaction energies at smaller system sizes compared to n-bond cluster models.

Ring Opening of Furan in Cluster Models of HZSM-5. Furan adsorbed in HZSM-5 can also be transiently protonated at the O1 site, leading to a neutral ring-opened product.[15] Figure 6 shows single-point and optimized reaction energies for the ring opening of furan in n-bond (Figure 6A) and delta clusters (Figure 6B) of HZSM-5.

Single-point energies for the ring-opening reaction appear to converge to ∼26 kcal/mol when $n \leq 7$ (Figure 6A). However, at $n = 8$ a significant increase by ≥ 40 kcal/mol is observed and persists until energies converge to ∼123.0 kcal/mol for values of $n \geq 9$. Upon optimization of the n-bond systems, this trend was not observed and energies quickly converged to ∼18.6 kcal/mol when $n \geq 7$ (Figure 6A). This behavior arises from the fact that the single-point studies on the ring-opened

structure lock the product into a configuration that experiences severe steric repulsion with the opposite side of the HZSM-5 channel. As such, once the value of n increases to complete the channel, the reaction energy jumps precipitously. This may be viewed as an inherent limitation of studying single-points; instead, we view this as a limitation of the n-bond cluster construction method, as described below.

A similar trend in single-point energies was not observed in cluster models constructed using multicentered spherical cutoffs (Figure 6B). Even at the smallest values of delta, single-point energy differences are >105 kcal/mol. When $\delta \geq 4.0$ Å, single-point energies converge to ∼123.4 kcal/mol and upon optimization energies converge to 18.5 kcal/mol at $\delta \geq 5.0$ Å (Figure 6B). A value of $\delta = 5.0$ Å corresponds to a system size of 34T in HZSM-5, significantly smaller than the n-bond system sizes necessary to converge energies. These delta-cluster results show that the multicentered spherical cutoffs method correctly constructed clusters that reveal the strong steric hindrance even for the smallest values of δ.

Our reaction energy for the ring opening of furan is significantly higher (by ∼7.5 kcal/mol) than the previously reported value of 11.0 kcal/mol.[15] However, the previous study used an embedded QM/MM approach to model HZSM-5. Although the total system size was 132T, only an 11T subunit surrounding the active site was modeled at the B3LYP/6-311G(d,p) model chemistry and the Universal Force Field (UFF) was used for the remaining MM layer.[15] On the basis of the excellent agreement between our computed reaction energies and those previously reported for the keto/enol tautomerization in HZSM-5 and HY at the same model chemistry,[4] we suggest that methodological differences may account for the discrepancy between reaction energies computed via quantum cluster and QM/MM techniques.

Generalized Protocol for Constructing Cluster Models of Zeolite Crystals. Here we describe a general procedure (Figure 7) for building zeolite clusters using the delta-cluster approach. Once one has identified a (i) reaction of interest, (ii) the zeolite type, and (iii) the acid site location, X-ray coordinates for the zeolite can be downloaded. The zeolite coordinates along with initial guesses for the reactant and product adsorbed guest geometries can be fed into the automated cluster-building script which uses the Schrödinger Python API. Initially a multicentered spherical cutoff of $\delta = 7$ Å should be applied to generate a large cluster, sufficient to further refine the guest molecule geometries (Figure 7A). This choice of a 7 Å cluster represents a balance between the need to start with a large initial cluster to capture as many effects as
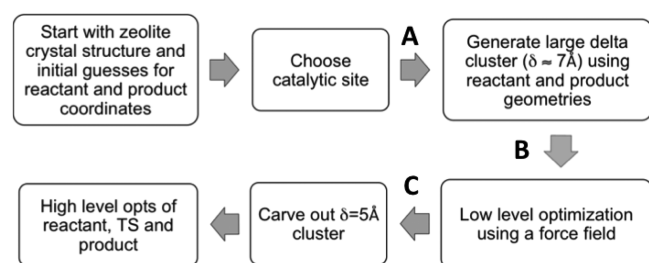
Figure 7. Flowchart illustrating a general procedure for constructing delta clusters of zeolites.

possible and the computational cost of preoptimization on such a large cluster. After the $\delta = 7$ Å "master" cluster is built, we suggest application of a low-level model (e.g., a generic force field such as UFF) to optimize the guest reactant and product geometries in a reasonable amount of time (Figure 7B). Once the low-level optimization is complete, the Python script is reapplied with a multicentered spherical cutoff of $\delta = 5.0$ Å to generate a smaller, converged production cluster (Figure 7C) for use in higher-level optimizations.

4. CONCLUDING REMARKS

We have studied the convergence of zeolite cluster models due to the importance of simulating zeolite-catalyzed reactions, the presence of long-range interactions in zeolite−guest systems, and the general utility of finite cluster models. We have studied four reactions as platforms for understanding how convergence of reaction energies may vary for neutral → neutral and neutral → charged processes. In particular, we have applied density functional theory calculations to compute reaction energies for acid-zeolite-catalyzed processes related to the conversion of biomass: (1) the keto−enol tautomerization of acetone in HZSM-5 and HY and (2) the protonation and ring opening of furan in HZSM-5. To investigate cluster convergence, we have compared two rather distinct methods for building successively larger clusters: one method (denoted "n-bond") is based on counting bonds from a catalytic site, while the other method (denoted "delta") applies multicentered spherical cutoffs from each guest reactant and product atom, as well as from the acid site.

We have investigated the convergence of reaction energies using both single-point calculations on clusters containing as many as 166 tetrahedral (T) atoms and optimizations on clusters with as many as 78 T atoms. For all the reactions we studied, the clusters generated with multicentered spherical cutoffs yield converged reaction energies with smaller system sizes than by counting framework bonds. This method employing a single length scale (5 Å) converges reaction energies to within chemical accuracy (±1 kcal/mol) and includes between 15 and 34 T atoms in the cluster depending on the process under study. On the basis of the general success of the delta-cluster method, we suggest a general protocol for generating such clusters for subsequent use in computational zeolite science.

■ ASSOCIATED CONTENT

Ⓢ Supporting Information

The following file is available free of charge on the ACS Publications website at DOI: 10.1021/cs501827p.

Grimme dispersion single-point energy corrections for all cluster models studied; Gibbs reaction energies for selected delta cluster models; nonoptimized structures for the 11 bond clusters of HZSM-5 and HY for each of the four reactions studied; optimized reactant and product structures for selected values of delta for the reaction systems studied (PDF)

■ AUTHOR INFORMATION

Corresponding Author
*E-mail: vaithee@chem.umass.edu.

Notes
The authors declare no competing financial interest.

■ ACKNOWLEDGMENTS

■ REFERENCES

(1) Corma, A. *Chem. Rev.* **1997**, *97*, 2373−2419.
(2) Baerlocher, C.; Meier, W. M.; Olson, D. H. *Atlas of Zeolite Framework Types*, 5th ed.; Elsevier: Amsterdam, The Netherlands, 2001; pp 184−185.
(3) Payra, A.; Dutta, P. K. In *Handbook of Zeolite Science and Technology*; Auerbach, S. M., Carrado, K. A., Dutta, P. K., Eds.; Marcel Dekker, Inc.: New York, NY, 2003; p 1.
(4) Migues, A. N.; Vaitheeswaran, S.; Auerbach, S. M. *J. Phys. Chem. C* **2014**, *118*, 20283−20290.
(5) Fermann, J. T.; Moniz, T.; Kiowski, O.; McIntire, T. J.; Auerbach, S. M.; Vreven, T.; Frisch, M. J. *J. Chem. Theory Comput.* **2005**, *1*, 1232−1239.
(6) Astala, R.; Auerbach, S. M. *J. Am. Chem. Soc.* **2004**, *126*, 1843−1848.
(7) Astala, R.; Auerbach, S. M.; Monson, P. A. *J. Phys. Chem. B* **2004**, *108*, 9208−9215.
(8) Astala, R.; Auerbach, S. M.; Monson, P. A. *Phys. Rev. B: Condens. Matter Mater. Phys.* **2005**, *71*, 14112−14127.
(9) Eichler, U.; Kolmel, C. M.; Sauer, J. *J. Comput. Chem.* **1997**, *18*, 463−477.
(10) De Moor, B. A.; Reyniers, M.-F.; Sierka, M.; Sauer, J.; Marin, G. B. *J. Phys. Chem. C* **2008**, *112*, 11796−11812.
(11) Maihom, T.; Pantu, P.; Tachakritikul, C.; Probst, M.; Limtrakul, J. *J. Phys. Chem. C* **2010**, *114*, 7850−7856.
(12) Namuangruk, S.; Pantu, P.; Limtrakul, J. *J. Catal.* **2004**, *225*, 523−530.
(13) Agarwal, V.; Conner, W. C.; Auerbach, S. M. *J. Phys. Chem. C* **2011**, *115*, 188−194.
(14) Agarwal, V.; Huber, G. W.; Conner, W. C.; Auerbach, S. M. *J. Catal.* **2010**, *269*, 53−63.
(15) Vaitheeswaran, S.; Green, S. K.; Dauenhauer, P.; Auerbach, S. M. *ACS Catal.* **2013**, *3*, 2012−2019.
(16) Bao, X. Y.; Sung, C. Y.; Snurr, R. Q.; Broadbelt, L. J. *ACS Catal.* **2012**, *2*, 350−359.
(17) Cheng, Y.-T.; Huber, G. W. *ACS Catal.* **2011**, *1*, 611−628.
(18) Cheng, Y.-T.; Jae, J.; Shi, J.; Fan, W.; Huber, G. W. *Angew. Chem., Int. Ed.* **2012**, *51*, 1387−1390.
(19) Czjzek, M.; Jobic, H.; Fitch, A. N.; T, V. *J. Phys. Chem.* **1992**, *96*, 1535−1540.
(20) van Koningsveld, H.; Jansen, J. C.; van Bekkum, H. *Zeolites* **1990**, *10*, 235−242.
(21) Becke, A. D. *J. Chem. Phys.* **1993**, *98*, 5648−5652.
(22) Krishnan, R.; Binkley, J. S.; Seeger, R.; Pople, J. A. *J. Chem. Phys.* **1980**, *72*, 650.

(23) Bochevarov, A. D.; Harder, E.; Hughes, T. F.; Greenwood, J. R.; Braden, D. A.; Philipp, D. M.; Rinaldo, D.; Halls, M. D.; Zhang, J.; Friesner, R. A. *Int. J. Quantum Chem.* **2013**, *113*, 2110−2142.

(24) Grimme, S.; Antony, J.; Ehrlich, S.; Krieg, H. *J. Chem. Phys.* **2010**, *132*, 154104.

(25) Boekfa, B.; Pantu, P.; Probst, M.; Limtrakul, J. *J. Phys. Chem. C* **2010**, *114*, 15061−15067.